# Organization and Orientation of Amphiphilic Push–Pull Chromophores Deposited in Langmuir–Blodgett Monolayers Studied by Second Harmonic Generation and Atomic Force Microscopy

**ARTICLE** *in* LANGMUIR · OCTOBER 2004

Impact Factor: 4.46 · DOI: 10.1021/la0491706 · Source: PubMed



**11 AUTHORS**, INCLUDING:

Aymeric Leray
French National Centre for Scientific Research
**36** PUBLICATIONS **266** CITATIONS
SEE PROFILE

Yann Le Grand
Université de Bretagne Occidentale
**71** PUBLICATIONS **426** CITATIONS
SEE PROFILE

Véronique Vié
Université de Rennes 1
**121** PUBLICATIONS **1,130** CITATIONS
SEE PROFILE

# Organization and Orientation of Amphiphilic Push−Pull Chromophores Deposited in Langmuir−Blodgett Monolayers Studied by Second Harmonic Generation and Atomic Force Microscopy

A. Leray,[†] L. Leroy,[†] Y. Le Grand,[†] C. Odin,[†] A. Renault,[†] V. Vié,[†] D. Rouède,*[,†] T. Mallegol,[‡] O. Mongin,[‡] M. H. V. Werts,[‡] and M. Blanchard-Desce[‡]

*GMCM, CNRS UMR 6626, Institut de Physique de Rennes, and SESO, CNRS UMR 6510, Institut de Chimie de Rennes, Université de Rennes 1, Campus de Beaulieu, 35042 Rennes Cedex, France*

*Received March 31, 2004. In Final Form: June 12, 2004*

Orientation and organization of two amphiphilic push−pull chromophores mixed with two phospholipids (dipalmitoylphosphatidylcholine and dioleoylphosphatidylcholine) in Langmuir−Blodgett (LB) monolayers are investigated by second harmonic generation. The LB monolayers have also been characterized by atomic force microscopy and UV−vis spectroscopy. The effective molecular orientations and hyperpolarizabilities of the chromophores are studied as a function of the phospholipid concentrations. The experimental results are discussed within the frame of a model of orientational distribution of the chromophores which gives the orientational mean angle and bounds on the orientational disorder. The mean orientation of the chromophores is found to be within 45−55° whereas their hyperpolarizability coefficients, measured with respect to quartz, are estimated to be in the range $(0.3-0.7) \times 10^{-27}$ esu taking account of the maximal orientational disorder.

## 1. Introduction

Amphiphilic push−pull chromophores are representative of a class of organic molecules that are of growing importance in nonlinear microscopy and particularly in second-harmonic generation (SHG) microscopy.[1−5] The main reasons for the interest in these dye molecules for biological imaging are (i) their large hyperpolarizability, which arises from the intense charge-transfer nature of their electronic transitions, and (ii) their ability to interact with the lipid membrane in order to image cellular membrane potential variations in living cells.[4−8] A key factor to control the efficiency of the SHG process using these chromophores in biological imaging concerns the orientation and the organization of the dye molecules in the membrane.[1,3] Phospholipid monolayers and bilayers formed using the Langmuir−Blodgett (LB) technique have long been used as models for biological membranes,[9,10] and the advantage of using this technique for the study of the molecular packing is the control of surface pressure and dye concentration.

Surface SHG of LB monolayers is a frequently used technique to characterize organization, average orientation, and second-order polarizability of chromophores.[11−17] Indeed, at interfaces the inversion symmetry is broken which leads to a nonvanishing macroscopic nonlinear susceptibility. Moreover, it has also been recognized that the polarization dependence of the SHG intensity can yield information about the average orientation of the dye molecules.[11−17]

Push−pull molecules used in the present study are amphiphilic derivatives[18] of hemicyanine dyes shown in Figure 1. The push−pull structure provides the molecular asymmetry that leads to large first-order hyperpolarizability. To favor asymmetrical incorporation in a hydrophilic−hydrophobic interface, a lipophilic/hydrophilic gradient is conferred to the chromophore by grafting two hexyl hydrophobic tails onto the donor end group and a zwitterionic hydrophilic part onto the acceptor moiety. As a result, the chromophore can be functionalized to be a molecular membrane marker.

In this work we investigated by SHG the organization and the orientation of two zwitterionic (**1**, **2**) compounds of amphiphilic dyes mixed with dipalmitoylphosphatidylcholine (DPPC) (saturated fatty acyl chains) and dioleoylphosphatidylcholine (DOPC) (containing a cis double bond in both fatty acyl chains) phospholipids. DPPC and DOPC were chosen for the two following main reasons.

* To whom correspondence should be addressed. E-mail: denis.rouede@univ-rennes1.fr.
[†] GMCM, CNRS UMR 6626, Institut de Physique de Rennes.
[‡] SESO, CNRS UMR 6510, Institut de Chimie de Rennes.

(1) Mertz, J. *C. R. Acad. Sci. Paris* **2001**, t. 2, Série IV, 1153−1160.
(2) Campagnola, P. J.; Loew, L. *Nat. Biotechnol.* **2003**, *21*, 1356−1360.
(3) Pons, T.; Moreaux, L.; Mongin, O.; Blanchard-Desce, M.; Mertz, J. *J. Biomed. Opt.* **2003**, *8*, 428−431.
(4) Blanchard-Desce, M. *C. R. Physique* **2002**, *3*, 439−448.
(5) Dombeck, D. A.; Blanchard-Desce, M.; Webb, W. W. *J. Neurosci.* **2004**, *24*, 999−1003.
(6) Millard, A. C.; Jin, L.; Lewis, A.; Loew, L. M. *Opt. Lett.* **2003**, *28*, 1221−1223.
(7) Peleg, G.; Lewis, A.; Linial, M.; Loew, L. M. *Proc. Natl. Acad. Sci. U.S.A.* **1999**, *96*, 6700−6704.
(8) Campagnola, P. J.; Mei-de Wei, A. Lewis; Loew, L. M. *Biophys. J.* **1999**, *77*, 3341−3349.
(9) Maget-Dana, R. *Biochim. Biophys. Acta* **1999**, *1462*, 109−140.
(10) Möhwald, H. In *Handbook of Biological Physics*; Lipowsky, Sackmann, E., Eds.; Elsevier: Amsterdam, 1995; Vol. 1, Chapter 4.
(11) Shen, Y. R. *Nature* **1989**, *337*, 519−525.
(12) Corn, R. M.; Higgins, D. A. *Chem. Rev.* **1994**, *94*, 107−125.
(13) Heinz, T. F.; Chen, C. H.; Ricard, D.; Shen, Y. R. *Phys. Rev. Lett.* **1982**, *48*, 478−481.
(14) Heinz, T. F.; Tom, H. W. K.; Shen, Y. R. *Phys. Rev. A* **1983**, *28*, 1883−1885.
(15) Eisenthal, K. B. *Chem. Rev.* **1996**, *96*, 1343−1360.
(16) Simpson, G. J.; Westerbuhr, S. G.; Rowlen, K. L. *Anal. Chem.* **2000**, *72*, 887−898.
(17) Brevet, P. F. In *Surface Second Harmonic Generation*, 1st ed.; Presses Polytechniques et Universitaires Romandes: Lausanne, 1996.
(18) Alain, V.; Blanchard-Desce, M.; Ledoux I.; Zyss, J. *Chem. Commun.* **2000**, 353−354.

10.1021/la0491706 CCC: $27.50 
Published on Web 08/20/2004

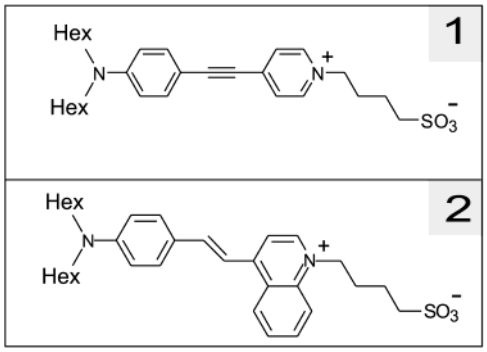


**Figure 1.** Molecular structures of the amphiphilic push−pull chromophores **1** and **2**.

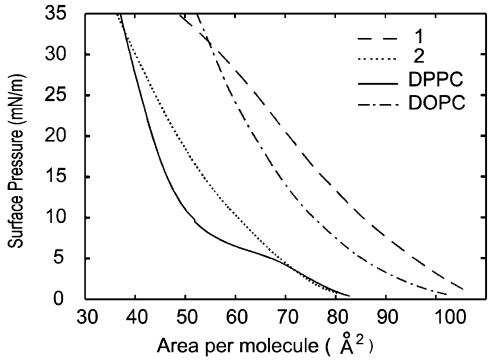


**Figure 2.** $\pi-A$ isotherms of DPPC, DOPC, and of pure compounds **1** and **2** at room temperature (20−22 °C).

Phospholipids with choline headgroups represent the most abundant phospholipid class in eukaryotic cells and, moreover, zwitterionic phospholipids DPPC and DOPC are expected to interact differently with chromophores as they form condensed and fluid phases, respectively, at room temperature. LB monolayers with different dye/lipid molar ratios, prepared under $\pi-A$ isotherm control, were first characterized by atomic force microscoopy (AFM) and UV−vis absorption spectroscopy. AFM images provide us with a straightforward insight of the mixture organization. Measurements of the SHG intensity generated by the LB monolayers were performed as a function of the input light polarization so as to determine the components of the macroscopic susceptibility $\chi^{(2)}$ tensor of the monolayer. Assuming that the molecules have a dominant hyperpolarizabity coefficient $\beta$ and that they are randomly distributed with the interface surface normal, an effective orientational angle $\theta_e$ can be deduced from the measurements of the nonlinear suceptibility coefficients using conventional analysis.[11−17] This angle corresponds to the most probable angle under the usually made assumption of a strongly peaked orientational distribution. In cases for which the orientational distribution $w(\theta)$ is not well represented by a $\delta$-function, the mean angle $\theta_o$ can be significantly different according to the orientational disorder. To evaluate the descrepancy between the measured orientational angle $\theta_e$ and the true mean angle $\theta_o$, an assumption on the form of the distribution function $w(\theta)$ has to be made. In this paper, we use a simple model of angular distribution $w(\theta)$ in order to quantify the effect of orientational disorder on the maximum discrepancies between $\theta_e$ and $\theta_o$. Moreover an estimation of the value of the dominant hyperpolarizability coefficient, obtained from comparison with quartz, is given.

## 2. Deposition and Characterization

**2.1. Film Deposition: $\pi-A$ Isotherms.** DPPC and DOPC phospholipids were purchased from Avanti Polar Lipids Alabaster and used as supplied. Each component of the dye/phospholipid mixture was dissolved in R.P. Normapur 99−99.4% chloroform at a concentration equal to $0.5 \times 10^{-3}$ mol/L. The mixture was prepared with the following dye/lipid molar ratios (0/1, 0.2/0.8, 0.4/0.6, 0.6/0.4, 0.8/0.2, 1/0). Both surface pressure−area isotherms and LB depositions were obtained by means of a computer-controlled Langmuir−Blodgett Nima model 112 Teflon trough (Nima Ltd., Coventry, U.K.) equipped with two movable Teflon barriers. The surface pressure was measured with a film balance controller (Nima surface pressure sensor, PS4) and the experimental setup was completed by a Nima dipper mechanism D1L for the deposition. Before the experiment was started, the trough was cleaned for 12 h with a 5% Decon 90 solution and rinsed at least three times with ultrapure deionized water, 18.2 MΩ·cm (UHQ ELGA, VivendiWater Systems, France). The Langmuir trough (80 $cm^2$ starting surface) was filled up by high-purity deionized water, and the different solutions were spread on the water subphase using a high precision Hamilton microsyringe. The appropriate volumes (26−32 $\mu$L) were adjusted to obtain an initial surface pressure between 0.4 and 1 mN/m. After solvent evaporation (≈10 min), the $\pi-A$ isotherm was measured at a compression speed of 1 cm/min with a controlled temperature of 20 °C. Monolayers were deposited onto freshly cleaved mica for AFM experiments and onto microscope glass slides for all optical studies due to residual SHG signal of mica substrates. Mica substrates were cleaned with ethanol, simply rinsed with 18.2 MΩ·cm deionized water, and cleaved. Glass substrates were cleaned and hydroxylated by immersion in a fresh "piranha" solution (1/3 volume of hydrogen peroxide (30%), 2/3 volume sulfuric acid (95−98%) and heated until oxygen bubbles freely formed). They were rinsed in 18.2 MΩ·cm deionized water and dried under nitrogen. Monolayers were compressed to the desired surface pressure (35 mN/m) and allowed to equilibrate (stabilization of the area after 1−2 h depending of the mixture). Then the transfer was performed by pulling freshly cleaved mica (or glass) through the air−water interface at a rate of 1 mm/min under constant surface pressure. Since the transfer took place on the two opposite sides of the glass plate, the coating was withdrawn from one side with optical paper impregnated with ethanol.

Compressional isotherms of DPPC, DOPC, and both dye monolayers at the air−water interface are shown in Figure 2. As previously reported,[19,20] in this temperature range DPPC isotherm is characterized by a shoulder where liquid-condensed and liquid-expanded phases coexist. DPPC is in a condensed state above 20 mN/m while DOPC exhibits an isotherm characteristic for one single liquid-expanded phase at all measured pressures. Compressional isotherms of pure dyes show a liquid-expanded behavior, and from the spreading isotherms, the mean molecular area $A$ was estimated equal to 49 and 37 $Å^2$ for pure compounds **1** and **2**, respectively, at 35 mN/m. For mixtures of compounds **1** or **2** realized with either DPPC or DOPC, compressional isotherms (not presented) show a similar behavior with a mean molecular area in the range 37−52 $Å^2$ at 35 mN/m (i.e., the isotherms of the mixture are bounded by the isotherms of the two corresponding constituents).

**2.2. AFM and UV−vis Absorption Measurements.** Atomic force microscopy images of the Langmuir−Blodgett

(19) Tamm, L. K.; McConnell, H. M. *Biophys. J.* **1985**, *47*, 105−113.
(20) Vié, V.; Van Mau, N.; Lesniewska, E.; Goudonnet, J. P.; Heitz, F.; Le Grimellec, C. *Langmuir* **1998**, *14*, 4574−4583.

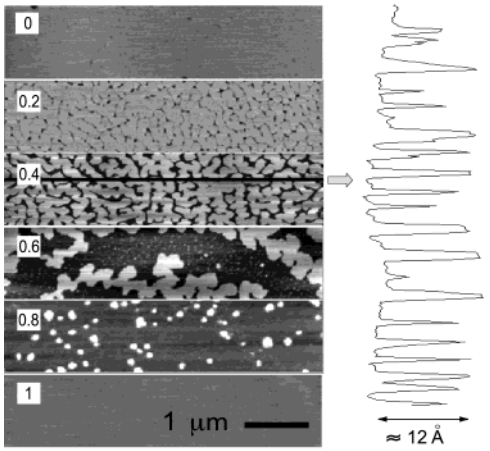


**Figure 3.** (a) 1.2 × 5 $\mu$m AFM topographical images of compound **1** mixed with DPPC on mica supported monolayers realized at 35 mN/m. Increasing dye/lipid molar ratio from the top to the bottom. (b) Cross section of the topographic image corresponding to the full line presented at a molar ratio equal to 0.4/0.6.

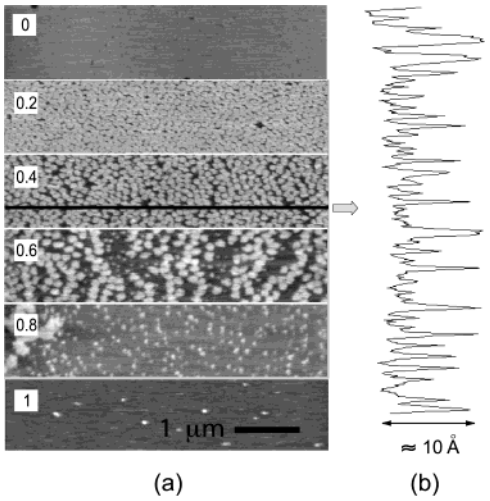


**Figure 4.** (a) 1.2 × 5 $\mu$m AFM topographical images of compound **2** mixed with DPPC on mica-supported monolayers realized at 35 mN/m. Increasing dye/lipid molar ratio from the top to the bottom. (b) Cross section of the topographic image corresponding to the full line presented at a molar ratio equal to 0.4/0.6.

monolayers deposited on mica substrates were obtained under ambient conditions using a Pico-plus atomic force microscope (Molecular Imaging, USA) operating in contact mode. Two scanners of 10 and 100 $\mu$m were used for measurements. Topographic images were acquired in constant force mode using silicon nitride tips with nominal spring constant of 0.12 N/m. Two LB films were deposited for each dye/lipid ratio, and distinct areas were imaged for each of the samples.

Typical topographic images realized for increasing ratios of compound **1** or **2** with DPPC are presented in Figures 3 or 4, respectively. The first image of both series, corresponding to a pure DPPC monolayer, reveals a uniform topography according to the single liquid condensed state behavior expected above 20 mN/m.[19] When the dye molar fraction increases, topographic images show only two distinct levels represented as bright and dark zones. A topographic profile of one of the mixed samples (0.4/0.6 in Figures 3b and 4b) reveals that bright areas appear higher than dark ones by about 10−12 Å. Morever

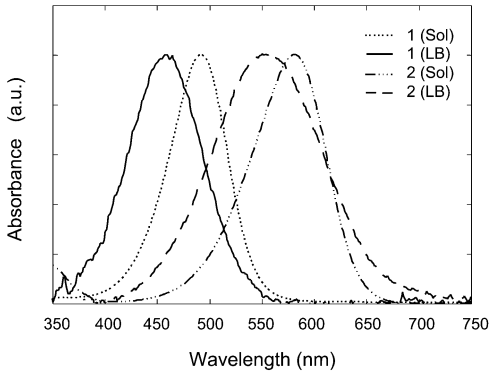


**Figure 5.** Normalized UV−vis absorption spectra of compounds **1** and **2** in LB films (LB) and in chloroform solution (Sol). The spectra of the LB films shown are those of the pure compounds.

the total bright area decreases with increasing dye/lipid molar ratio. All these observations allow us to attribute brightness to the lipid and darkness to the dye, and strongly suggest a demixing between DPPC and compound **1** or **2**. However the form of the DPPC domains looks quite different for the two dyes. They have an arborescent-like contour and globular structures in the presence of compounds **1** and **2**, respectively. Topographic images of pure compounds **1** and **2** are flat within the resolution of the AFM as shown by the last image of both series. For all films formed from a mixture of dye and DPPC, the height of the monolayer was estimated to be about ≈20 Å by locally removing the molecules from the substrate (the surface was scratched with the probe at high speed and forces for several minutes). Monolayers of compounds **1** and **2** mixed with DOPC at the same molar ratios show no visible demixion in the topographic and friction imaging modes (uniform images not presented). Even so, we cannot exclude the presence of very small domains of dye which may be hidden by the fluidity of DOPC (in liquid expanded phase).

UV−visible absorption spectra of compounds **1** and **2** in chloroform solution and in LB films were recorded at normal incidence using a Jasco V-570 double-beam spectrophotometer. A clean glass slide was used as a reference. Figure 5 shows that absorption spectra of both dyes deposited in LB films exhibit a blue shift of the absorption band compared with that of the corresponding chloroform solutions. Indeed, it is well-known that variations in the microenvironment of the dye can significantly modify the absorption spectra and more generally the linear and nonlinear optical properties, due to solvatochromic effects.[21,22] The observed blue shift is probably also associated to the formation of H-aggregates, which is often reported in hemicyanine LB monolayers for such high surface pressure.[21,23,24] Any significant variations of the maximum absorption wavelength were detected (within the spectral resolution of our measurements) as a function of the dye/lipid molar ratio. However in the frame of our SHG study, these absorption spectra could allow correction of the measured hyperpolarizabilities accounting for resonant effects.

## 3. SHG Study

**3.1. Experimental Setup.** The laser source used in the experiment was a picosecond Nd:YAG laser (Quantel

(21) Mishra, A.; Behera, R. K.; Behera, P. K.; Mishra, B. K.; Behera, G. B. *Chem. Rev.* **2000**, *100*, 1973−2011.
(22) Laage, D.; Thompson, W. H.; Blanchard-Desce, M.; Hynes, J. T. *J. Phys. Chem. A* **2003**, *107*, 6032−6046.
(23) Han, K.; Ma, S.; Lu, X. *Opt. Commun.* **1995**, *118*, 74−78.
(24) Ma, S.; Lu, X.; Han, K.; Liu, L.; Wang, W.; Zhang, Z.; Zhangb, Z.; Zhongb, J. *Thin Solid Films* **1995**, *256*, 215−219.

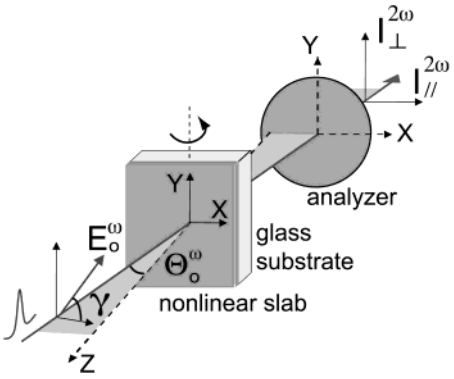


**Figure 6.** Schematic of the experiment. The direction of the polarization $\mathbf{E}_o^{\omega}$ of the incident beam is controlled with a half-wave plate (not represented). The SHG signal was measured as a function of the input polarization angle $\gamma$ of the input electric field $\mathbf{E}_o^{\omega}$ and the $XZ$ plane of incidence, $Z$ is the surface normal. The direction of the analyzer was fixed in either the $X(\|)$ or $Y(\perp)$ direction.

France, YG501, 30 ps, 20 Hz) emitting at $\lambda = 1.06\,\mu$m. The laser beam was passed through a set of fixed polarizers followed by a rotating half-wave plate in order to turn continuously the input electric field $\mathbf{E}_o^{\omega}$ from $X$ (parallel to the plane of incidence $\|$) to $Y$ (perpendicular to the plane of incidence $\perp$) within a precision of about $^1/_2°$ (see Figure 6). The transmitted intensity from the LB film was passed through a high-density IR filter (ND10) for removing the laser pump. The second-harmonic signal was resolved into its $X$ or $Y$ polarization component with a rotating analyzer and then detected with a fast photomultiplier tube (H5783-01, Hamamatsu) connected to a 50 Ω input impedance of 2.5 Gs/s digital oscilloscope (TDS 620B, Tektronix) used as a sampler and averager (over 200 laser pulses). The films were positioned on a rotation stage in order to adjust the angle of incidence $\Theta_o^{\omega}$ and always irradiated with the nonlinear slab facing toward the incident pump beam. SHG intensity from LB films was measured as function of the angle of polarization $\gamma$ of the input electric field $\mathbf{E}^{\omega}$ relative to the $XZ$ plane of incidence.

**3.2. Theoretical Model.** As a rule, second harmonic fields $E^{2\omega}$ originate from a surface nonlinear polarization $P^{2\omega}$ induced by mixing of intense electric fields $E^{\omega}$ at $\omega$ in the medium, as described by the following tensorial equality

$$P_i^{2\omega} = \chi_{ijk}^{(2)}\, E_j^{\omega}\, E_k^{\omega} \tag{1}$$

where $\chi^{(2)}$ is the surface macroscopic nonlinear susceptibility tensor and subscribes $i,j,k$ refer to the laboratory coordinates ($X$, $Y$, $Z$). The SHG intensities produced from a thin slab of nonlinear material between two linear media have been theoretically derived in the pioneering work of Bloembergen and Pershan.[25] In this meaningful work, the expressions of the perpendicular $E_{\perp}^{2\omega}$ and parallel $E_{\|}^{2\omega}$ components of the $2\omega$ electric fields transmitted by the slab into the substrate are given as a function of the induced nonlinear polarization $P^{2\omega}$ in the slab

$$E_{\perp}^{2\omega} = \tilde{f}_Y\, P_Y^{2\omega}; \qquad E_{\|}^{2\omega} = \tilde{f}_X\, P_X^{2\omega} + \tilde{f}_Z\, P_Z^{2\omega} \tag{2}$$

The coefficients $\tilde{f}$ in the above equation are usually considered as nonlinear Fresnel coefficients.[16,26] They depend on the refractive indices of the slab $n_s^{2\omega}$ and of the glass substrate $n_g^{2\omega}$ at $2\omega$ for a fixed angle of incidence $\Theta_o^{\omega}$ of the input beam. It is worthwhile to notice than the

(25) Bloembergen, N.; Pershan, P. S. *Phys. Rev.* **1962**, *128*, 606−622.

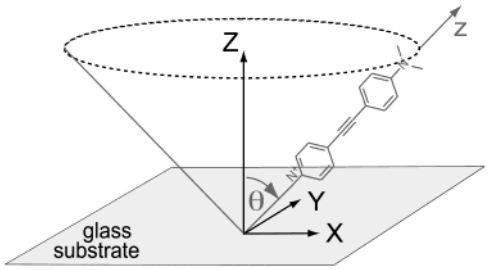


**Figure 7.** Model of random azimuthal orientation of the dye molecules in the LB film. $\theta$ is the angle between the surface normal laboratory axis $Z$ and the aromatic molecular axis $z$ active in SHG, which is supposed to be almost parallel to the principal axis corresponding to $\beta_{z,z,z}^{(2)}$.

electric fields considered in eqs 1 and 2 are given in the slab and in glass, respectively. To give an explicit expression of the nonlinear transmitted intensity as function of the input one, linear refractive processes have to be taken into account at the air/slab and glass/air interfaces for the $\omega$ and $2\omega$ waves, respectively. Neglecting these coefficients precludes extracting any correct value for the nonlinear coefficients as well as for the orientation of the chromophores.[26,27] The electric field components $E_i^{\omega}$ in the slab can then be explicitly written as a function of the amplitude of the input electric field $E_o^{\omega}$ and of the polarization angle $\gamma$ at a given angle of incidence $\Theta_o^{\omega}$ (see Figure 6)

$$E_X^{\omega} = f_X^{\omega} \cos\gamma \cos\Theta_o^{\omega}\, E_o^{\omega}$$

$$E_Y^{\omega} = f_Y^{\omega} \sin\gamma\, E_o^{\omega}$$

$$E_Z^{\omega} = f_Z^{\omega} \cos\gamma \sin\Theta_o^{\omega}\, E_o^{\omega} \tag{3}$$

In the above equation, $f^{\omega}$ stands for linear Fresnel transmission coefficients at the air/slab interface. They only depend on the refractive index of the slab $n_s^{\omega}$ at $\omega$ and of $\Theta_o^{\omega}$ and can be found in standard textbooks.[28] The SHG intensity $I^{2\omega} \sim |E_{\perp,\|}^{2\omega}|^2$ can be derived using eq 2 if the macroscopic nonlinear susceptibility $\chi^{(2)}$ is known. Indeed $\chi^{(2)}$ is itself related to the microscopic hyperpolarizability tensor $\beta^{(2)}$ of the nonlinear molecules through a coordinate transformation from the molecular ($x,y,z$) to the laboratory ($X,Y,Z$) coordinate systems and through an orientation average over the number of active molecules $N_s$ per unit surface. For the chromophores under study, we assumed that $\beta^{(2)}$ is dominated by the axial coefficient $\beta_{z,z,z}^{(2)} \equiv \beta$ associated with the push−pull molecular axis $z$.[18] Moreover, assuming that the azimuthal angle of the molecules is randomly distributed in the $XY$ plane with an angle $\theta$ about the interface normal axis $Z$ (see Figure 7), the only nonvanishing components of $\chi^{(2)}$ reduces to $\chi_{ZZZ}^{(2)}$ ($=\chi_{33}$) and $\chi_{iiZ}^{(2)} = \chi_{iZi}^{(2)} = \chi_{Zii}^{(2)}$ ($=\chi_{15}$) for $i = X$ or $Y$[14] with

$$\chi_{33} = N_s \beta \langle \cos^3\theta \rangle$$

$$\chi_{15} = \frac{1}{2} N_s \beta \langle \cos\theta \sin^2\theta \rangle$$

$$= \frac{1}{2} N_s \beta (\langle \cos\theta \rangle - \langle \cos^3\theta \rangle) \tag{4}$$

where $N_s$ is the surface density of active chromophores. The brackets $\langle\rangle$ indicates an orientational average over the distribution of molecular orientations $w(\theta)$, which is

defined as follows

$$\langle \cos^n \theta \rangle = \frac{\int_0^\pi \cos^n \theta \; w(\theta) \sin \theta \; d\theta}{\int_0^\pi w(\theta) \sin \theta \; d\theta} \qquad (5)$$

The sin $\theta$ term accounts for the metrics of the spherical coordinates, and the integration can be usually simplified by integrating over the new variable $z = \cos \theta$.

Using eqs 1−4, the transmitted SHG intensity $I_{\perp,\parallel}{}^{2\omega} = |f_{\perp,\parallel}{}^{2\omega} E_{\perp,\parallel}{}^{2\omega}|^2$ can be derived as function of the incident one $I^\omega = |E_o{}^\omega|^2$

$$I_\perp{}^{2\omega} = |f_\perp{}^{2\omega}|^2 |a_1 \chi_{15} \sin 2\gamma|^2 I^\omega I^\omega$$

$$I_\parallel{}^{2\omega} = |f_\parallel{}^{2\omega}|^2 |\chi_{15}(a_2 \cos^2 \gamma + a_3 \sin^2 \gamma) + \chi_{33} a_4 \cos^2 \gamma|^2 I^\omega I^\omega \qquad (6)$$

where $f_\perp{}^{2\omega}$ and $f_\parallel{}^{2\omega}$ are linear Fresnel coefficients which account for refraction of the second harmonic fields $E_{\perp,\parallel}{}^{2\omega}$ at the glass/air exit interface and $a_i$ are coefficients which depend on $f_i$, $\tilde{f}_i$, and $\Theta_o{}^\omega$. Equation 6 is the polarization dependence of the SHG intensity from a nonlinear slab usually found in the literature.[12,16,26] Fitting the experimental data of $I_\perp{}^{2\omega}(\gamma)$ and $I_\parallel{}^\omega(\gamma)$ with use of eq 6 allows determination of the ratio $\chi_{33}/\chi_{15}$. From this ratio, we deduce the *orientation parameter D*, and subsequently *an effective angle* $\theta_e$, both defined as[29]

$$D = \frac{\langle \cos^3 \theta \rangle}{\langle \cos \theta \rangle} = \frac{\chi_{33}/\chi_{15}}{2 + \chi_{33}/\chi_{15}} = \cos^2 \theta_e \qquad (7)$$

As can be seen, $\theta_e$ nearly corresponds to the angle of maximum probability $\theta_o$ when the distribution function $w(\theta)$ is very narrow. Otherwise, when the angular distribution is not strongly "peaked", the effective angle $\theta_e$ will depend on the shape and of the width of the distribution function $w(\theta)$ which describes the orientational disorder.

Correspondingly, we propose to define an effective hyperpolarizability coefficient $\beta_e$ by one of the following relations

$$\chi_{33} = N_s \beta_e \cos^3 \theta_e = N_s \beta_e D^{3/2}$$

$$\chi_{15} = \frac{N_s \beta_e}{2} \cos \theta_e \sin^2 \theta_e = \frac{N_s \beta_e}{2} D^{1/2}(1 - D) \qquad (8)$$

As $N_s$ and $D$ are known from chromophore surface area in LB monolayers and SHG intensity, respectively, $\beta_e$ can be derived if $\chi_{33}$ or $\chi_{15}$ can be measured by calibration from a known nonlinear material (see next section). The effective parameters $\theta_e$, $\beta_e$ coincide respectively with the angle of maximum probability $\theta_o$ and with the true hyperpolarizability $\beta$ only if the orientational disorder is small. Conversely it is known, for instance,[29] that for sufficiently broad Gaussian distribution function wrapped over [0, $\pi$], the effective angle $\theta_e$ would converge toward a "magic angle" 39.2°.

(26) Dick, B.; Gierulski, A.; Marowsky, G.; Reider, G. A. *Appl. Phys. B* **1995**, *38*, 107−116.
(27) Flueraru, C.; Schrader, S.; Zauls, V.; Dietzel, B.; Motschmann, H. *Opt. Commun.* **2000**, *182*, 457−466.
(28) Born, M.; Wolf, E. *Principles of Optics*, 6rd ed.; Pergamon Press: Oxford, 1993; p 40.
(29) Simpson, G. J.; Rowlen, K. L. *J. Am. Chem. Soc.* **1999**, *121*, 2635−2636.

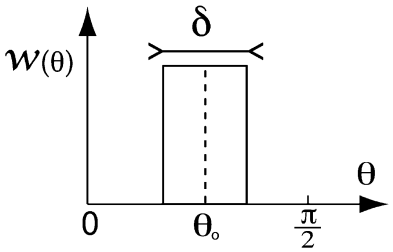


**Figure 8.** Orientational distribution function with mean orientation angle $\theta_o$ and width $\delta$. The orientation angle $\theta$ is restricted to [0, $\pi$/2] for amphiphilic monolayers.

However, in the present work, we consider monolayers of functionalized amphiphilic molecules deposited on a substrate whose surface has hydrophilic affinity, and in such conditions, head to tail organization of the molecules is highly improbable. Then, it is justified to quantify the effect of orientational disorder on the effective angle and hyperpolarizability coefficient using angular distributions that are limited to [0, $\pi$/2] and the considerations developed in ref 29 cannot be applied. The object of the next section is to derive relationships between the parameters of the angular distribution $w(\theta)$ and the effective angle $\theta_e$ and hyperpolarizability $\beta$ in the frame of a simple model.

**3.3. Effective Orientation Angle and Disorder.** Usually the orientational distribution function $w(\theta)$ is conventionally approximated by a Gaussian distribution function, $w(\theta) \sim \exp(-(\theta - \theta_o)^2/2\sigma^2)$ in which $\theta_o$ is the mean tilt angle and $\sigma$ the width of the distribution. Obviously when $\sigma \ll 1$, the effective angle $\theta_e \approx \theta_o$. However, strictly speaking, the Gaussian approximation is only justified when $\sigma$ is small enough so that $\theta$ is confined within [0, $\pi$/2]. If that is not the case, the Gaussian has to be wrapped[29] into the interval of study [0, $\pi$/2] and no more simple relationship between $\theta_e$ and $\theta_o$ exists. Here, we consider the more tractable uniform distribution (see Figure 8) which gives analytical expressions. It is important to note that the resulting trends (see Figure 9) appear to be quite representative of the general behavior found in the case of the more usual (but not analytically tractable) distribution functions such as the truncated or wrapped Gaussians. This point has been numerically verified, but a detailed presentation is out of the scope of this work.

The uniform distribution $w(\theta)$ is defined by two parameters, its width $\delta$ and its center $\theta_o$, where $0 \le \theta_o - \delta/2 \le \theta_o + \delta/2 \le \pi/2$.

Note that the usual conical distribution where the main axis is uniformly distributed within a cone of half-angle $\delta$ is obtained when $\theta_o - \delta/2 = 0$. The orientational parameter $D$, given by eq 7, can be derived from integration of eq 5 for $n = 1$ and $n = 3$.

$$D(\delta, \theta_o) = \frac{1}{2}(1 + \cos \delta \cos 2\theta_o) \qquad (9)$$

The parameters $\delta$ and $\theta_o$ should verify: (i) for $\theta_o$ within [0, $\pi$/4], $0 \le \delta \le 2\theta_o$; (ii) for $\theta_o$ within [$\pi$/4, $\pi$/2], $0 \le \delta \le \pi - 2\theta_o$. $D$ is bounded within $0 \le D \le 1$ and is an even function of $\delta$. When the distribution width is very small ($\delta \ll 1$), we obtained $D \approx \cos^2 \theta_o - (\delta^2/4) \cos 2\theta_o$ and it is easily verified that $D \to \cos^2 \theta_o$ when $\delta \to 0$. Figure 9 shows the relationship between $\delta$ and $\theta_o$ at a given $D$. It is noteworthy that the "constant $D$" lines are almost vertical, indicating that the mean angle $\theta_o$ is well defined by the value of $D$. If $D = 1/2$, then $\theta_o$ is exactly 45° whatever the distribution width $\delta$. Graphs of Figure 9 clearly demonstrate that $D$ is not sufficient to characterize the

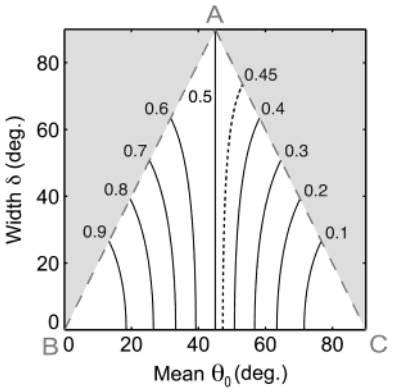


**Figure 9.** Distribution width $\delta$ as a function of mean angle $\theta_o$ at given orientation parameter $D$ (numbers in the figure) for the uniform angular distribution defined in the text (see Figure 8). The dashed line corresponds to the experimentally measured $D \approx 0.46$ value. Point A corresponds to the uniform distribution within $[0, \pi/2]$. Points B and C correspond to $w(\theta) = \delta(\cos\theta - 1)$ and $w(\theta) = \delta(\cos\theta)$, respectively, where $\delta$ is here the Dirac function. To keep the shape of the uniform distribution function, the region of variation of the mean $\theta_o$ and width $\delta$ are limited to a triangle, drawn in bold dashed lines.

orientational disorder $\delta$, as exemplified by the curve $D = 1/2$ where all disorder gives the same $D$ value.

It can be shown[30] that $\beta_e$ always underestimates $\beta$, whatever the angular distribution function $w(\theta)$ as long as the angular variation is limited to $[0\ \pi/2]$. For the uniform and wrapped Gaussian distributions considered above, the relative underestimation $(\beta - \beta_e)/\beta$ is no more than ≈30% and ≈40%, respectively. This shows that measurements of hyperpolarizability on LB films using the SHG technique can be obtained with a good confidence interval.

## 4. Results and Discussion

As a preliminary experiment, we checked that the SHG intensity was kept constant, for all the LB samples, as the substrate was rotated around its surface normal. This demonstrates that the chromophores have random azimuthal orientations, thus justifying the form of the susceptibility tensor used in the model developed above.

The polarization dependence of the SHG intensity is shown in Figure 10 for LB films obtained from a mixture of compounds **1** and **2** with DPPC at a dye/lipid molar ratio equal to 0.4/0.6. The SHG data were fitted using eq 6 with a least-squares procedure so as to find $\chi_{33}/\chi_{15}$. The Fresnel coefficients $f_{\perp,\parallel}$, $f_i$, and $\tilde{f}_i$ involved in eq 6 are given in ref 26 as a function of the glass $n_g^{2\omega}$ and slab $n_s^{\omega}$, $n_s^{2\omega}$ indices respectively, for a fixed angle of incidence $\Theta_o^{\omega}$. This angle was fixed to $\Theta_o^{\omega} = 70°$, because it nearly gives the maximum intensity for all the films studied. Considering the fineness of the nonlinear slab (thickness $t \approx$ 1 nm), the approximation $n_s^{\omega} = n_s^{2\omega} = n_s$ is usually made.[26] The index of refraction $n_g^{2\omega}$ was measured with a Pulfrich refractometer to be equal to 1.5126 at $\lambda = 589$ nm and was extrapolated to $n_g^{2\omega} = 1.5153$ at $\lambda = 532$ nm using a standard dispersion model for glass. The refractive index $n_s$ can be obtained from the ratio $I_{\perp}^{2\omega}(\gamma = 45°)/I_{\parallel}^{2\omega}(\gamma = 90°)$ at a fixed $\Theta_o^{\omega}$ since this ratio does not depend on the nonlinear susceptibility (see eq 6). We found $n_s = 1.30 \pm 0.02$ and $n_s = 1.39 \pm 0.02$ for the mixtures of compounds **1** and **2** with DPPC respectively realized at the molar ratio 0.4/0.6. As shown by Figure 10 the good agreement between experiment and theory indicates that the proposed SHG model is well suited for this system. We found

(30) Leray, A.; Rouède, D.; Odin, C.; Blanchard-Desce, M.; Le Grand. Y. To be submitted to *Opt. Commun.*

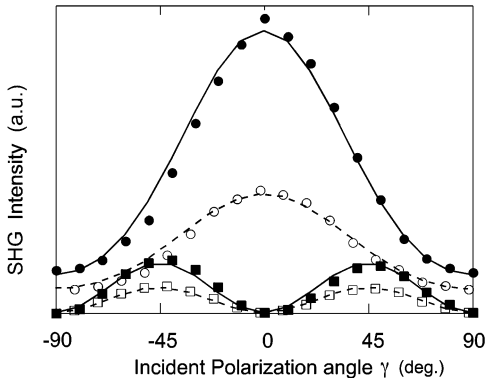


**Figure 10.** Polarization dependence of the $I_{\parallel}^{2\omega}$ (circles) and $I_{\perp}^{2\omega}$ (squares) SHG intensity from LB films realized from a mixture dye/DPPC (=0.4/0.6) of compounds **1** (○, □) and **2** (●, ■) for $\Theta_o^{\omega} = 70°$. The dots correspond to the experimental data while the full line is drawn from the best fit obtained from eq 6 (the SHG intensity for compound **2** is enhanced by a factor of 10 compared to the one of compound **1** for the same IR intensity).

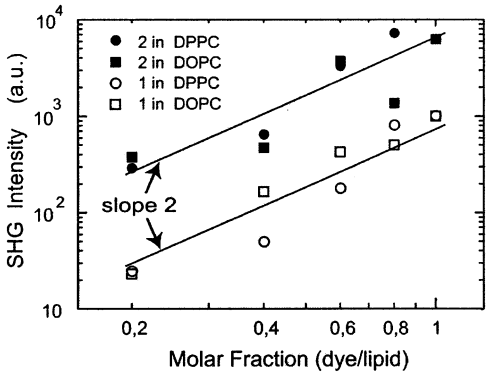


**Figure 11.** SHS intensity $I_{\parallel}^{2\omega}$ for compounds **1** and **2** in DPPC and DOPC as function of the molar fraction obtained at $\pi = 35$ mN/m for $\Theta_o^{\omega} = 70°$, $\gamma = 0°$: compound **1** in DPPC (○) and in DOPC (□); compound **2** in DPPC (●) and in DOPC (■).

$D = 0.43 \pm 0.02$ and $D = 0.50 \pm 0.02$ for mixtures of compounds **1** and **2** with DPPC, respectively, which leads to $\theta_e = 49 \pm 1°$ and $\theta_e = 45 \pm 1°$. According to Figure 9, the mean angle lies within $\theta_o \approx 47-53°$ for compound **1**, and the maximal dispersion can be ≈70°. Similarly for compound **2**, $\theta_o \approx 45°$, and a maximal dispersion as high as ≈90° is possible. Since the effective angle is always close to ≈45° for these dyes, our SHG measurements are quite insensitive to orientational disorder $\delta$.

To probe the dye/lipid molar fraction dependence on the tilt angle, SHG measurements were performed for films prepared with different mixtures of compounds **1** or **2** with DPPC or DOPC in the same molar ratios as the ones realized for the AFM measurements. As proof of the good insertion of the dye into the monolayer, we verified the expected quadratic dependence of the SHG intensity as a function of the dye/lipid molar fraction, for $\gamma = 0°$ (see Figure 11). It is worth mentioning that such a behavior excludes any significant change of the molecular environment associated with the phospholipids which would produce modifications of the hyperpolarizability coefficient.

The orientation parameter $D$ and the effective tilt angle $\theta_e$ derived from the polarization dependence SHG intensity are reported in Table 1.

The values of $D$ are ranging from 0.41 to 0.48 for compound **1** and from 0.45 to 0.52 for compound **2**. Then the corresponding mean angles $\theta_o$ are restrained within

**Table 1. Orientational Parameter *D* and Effective Tilt Angle $\theta_e = D^{1/2}$ for LB Films Realized from a Mixture of Compounds 1 or 2 with the Two Lipids for Molar Ratios Dye/Lipid Ranging from 1 to 0 at $\pi = 35$ mN/m and for $\Theta_o^{\omega} = 70°$ [a]**

| molar fraction dye/lipid | compound **1** | | | | compound **2** | | | |
|---|---|---|---|---|---|---|---|---|
| | DPPC | | DOPC | | DPPC | | DOPC | |
| | *D* | $\theta_e$ | *D* | $\theta_e$ | *D* | $\theta_e$ | *D* | $\theta_e$ |
| 1/0 | 0.41 | 50 | 0.41 | 50 | 0.45 | 48 | 0.45 | 48 |
| 0.8/0.2 | 0.45 | 48 | 0.48 | 46 | 0.53 | 43 | 0.45 | 48 |
| 0.6/0.4 | 0.48 | 46 | 0.46 | 47 | 0.50 | 45 | 0.48 | 46 |
| 0.4/0.6 | 0.43 | 49 | 0.41 | 50 | 0.50 | 45 | 0.45 | 48 |
| 0.2/0.8 | | | 0.41 | 50 | 0.48 | 46 | 0.52 | 44 |

[a] *D* is obtained from the ratio $\chi_{33}/\chi_{15}$ giving the best fit of the SHG data with the theoretical expression given by eq 6 and is obtained with an accuracy $\Delta D \approx \pm 0.02$. Prior to the determination of *D*, the index of refraction has been measured for each film with the method described in the text (the values are not presented).

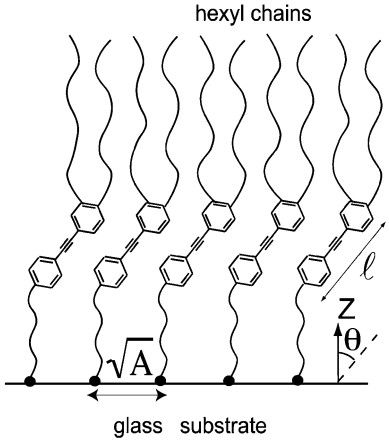


**Figure 12.** Proposed scheme of molecular packing of the chromophores in the LB film. The circles represent the zwitterionic hydrophilic headgroups. The projected area is $A \approx (l \sin \theta)^2$.

(45−55°) (see Figure 9) with a large indetermination on $\delta$. For compound **2** we recover a similar value of $\theta_e$ as previously measured (45−50°) with a quite different approach[3] based on giant unilamellar vesicles (GUVs) prepared from DOPC, supporting the relevance of the LB method in modeling lipidic membranes. It can also be noticed that for any phospholipid and molar fraction, orientational parameters remain nearly constant. This results suggest a self-organization of the dye in the LB films, in accordance with the AFM results and may be interpreted as an effect of chromophore demixion (that is formation of H-aggregates of dye molecules) independently of the phospholipid concentration.

In this context it is interesting to consider a simple model of dye packing in the case of demixion (see Figure 12). In that model the mean area per dye in the conditions of deposition ($A \sim 40-50$ Å$^2$ at 35 mN/m) is compatible with a packing mainly limited by the two hexyl chains (cross-sectional area of one all-trans hexyl chain of ≈21 Å$^2$ [32]). We thus expect that the rigid aromatic part of the chromophore takes a molecular orientation which gives, on average, the same projected area *A*. Considering that the length of the rigid part of the chromophore is about $l \sim 9-10$ Å[22] and using $(l \sin \theta_o)^2 = A$, we obtain $\theta \sim 40-50°$, which is fully compatible with the experimental values measured by SHG.

Absolute values of surface nonlinear susceptibility coefficients $\chi_{15}$ and $\chi_{33}$ can be obtained by calibration of the previous SHG intensity measurements with a reference nonlinear crystal. In this work, the value of $\chi_{15}$ was estimated relative to the bulk coefficient $\chi_{11} = 1.9 \times 10^{-9}$ esu[3131] of a 4 mm thick *Y*-cut quartz plate using the Maker fringe method.[33,34] We found $\chi_{15} = 1.2 \times 10^{-14}$ esu and $2.5 \times 10^{-14}$ for compounds **1** and **2**, respectively. Using eq 8 and considering that $N_s = 1/A$, the hyperpolarizability coefficients are $\beta_e = 0.3 \times 10^{-27}$ esu and $0.5 \times 10^{-27}$ esu for compounds **1** and **2**, respectively. Details of the calculation taking account of all the Fresnel corrections can be found in ref 26. As previously mentioned, the true hyperpolarizability coefficient $\beta$ is always underestimated by the measure of $\beta_e$ with a maximum underestimation of approximatively 30−40%. These hyperpolarizability coefficients are quite comparable with those of other hemicyanines[35] usually measured by hyper-Rayleigh scattering (HRS) in solution. However comparison with measurements in solution has to be made with caution because $\beta$ is very sensitive to the environment and extrapolation to anisotropic condensed phases is not easy. However any comparison with EFISH technique measuring $\mu\beta$ in solution (where $\mu$ is the dipole moment of the molecules) has to be made with caution for two reasons: (i) $\mu$ has to be determined separately and (ii) both $\mu$ and $\beta$ are very sensitive to the environment and extrapolation to a condensed phase is hazardous. Consequently the LB method appears to be quite a good tradeoff between control of parameters (pressure, concentration, ...) and biologically relevant environment.

## 5. Conclusion

The nonlinear quadratic optical properties of two new amphiphilic push−pull chromophores mixed with phospholipids (DPPC and DOPC) in Langmuir−Blodgett (LB) films have been investigated by SHG. The effective molecular orientations and hyperpolarizabilites of the chromophores derived from a standard optical model, and assuming random azimuthal orientation and single component of the nonlinear polarizability, have been shown to be quite independent of the phospholipid concentrations. These results, together with AFM observations, have supported the assumption of clustering of these dyes into the phospholipids. A simple model of molecular angular distribution $w(\theta)$, within $[0, \pi/2]$, has allowed us to quantify maximal deviations between the effective measured values and the true ones. We found that the mean orientation $\theta_o$ is within (45−55°), although the orientational disorder remains quite undetermined. The true hyperpolarizability coefficient $\beta^{(2)}$ was estimated to be in the range $(0.3-0.7) \times 10^{-27}$ esu at 1064 nm fundamental wavelength. More insight about orientational disorder of our nonlinear chromophores, which are also fluorescent,[4] could be achieved by combining SHG and fluorescence techniques, since the latter would permit to adress different order parameters. Moreover considering the voltage sensitivity of these dyes, such functionalized chromophores belong to the most promising membrane potential sensors for neurophysiological imaging.[3,5]

**Acknowledgment.** The authors are grateful to Dr. F. Artzner for participating in helpful discussions.

LA0491706

(31) Shen, Y. R. *The Principles of Nonlinear Optics*; Wiley: New York, 1992; Chapter 7.
(32) Israelachvili, J. N. *Intermolecular and surface forces*; Academic Press: London, 1997; Chapter 17.
(33) Maker, P. D.; Nisenhoff, R. W. M.; Savage, C. M. *Phys. Rev. Lett.* **1962**, *8*, 121−122.
(34) Jerphagnon, J.; Kurtz, S. K. *J. Appl. Phys.* **1970**, *41*, 1667−1681.
(35) Zyss, J.; Ledoux, I.; Nicoud, J. F. In *Molecular Nonlinear Optics*; Zyss, J., Ed.; Academic Press: New York, 1994; Chapter 4.